

<연구논문>

Interdiffusion in Pd/Cu Multilayered Film and Its Thermal Stability

In Joon Jeon*, Young Pak Lee** and Jae-Hwa Hong†

Department of Physics, Pohang Institute of Science and Technology, Pohang 790-784

†Research Institute of Industrial Science and Technology, P.O. Box 135, Pohang 790-600

(Received January 10, 1994)

Pd/Cu 다층박막의 상호확산 및 열안전성

전인준* · 이영백** · 홍재화†

포항공과대학 물리학과, †산업과학기술연구소 기초과학연구분야

(1994년 1월 10일 접수)

Abstract — In thin films, diffusion phenomena play an important role for the growth process, and in the understanding of the mechanical, electrical and magnetic properties. The change in the concentration profile due to the interdiffusion by annealing was investigated using AES depth-profiling technique on Pd/Cu multilayered films. It was observed that the initial concentration distributions, which were almost rectangular in the unheated samples, were changed into sinusoidal ones in the annealed films at various temperatures. The concentration-independent interdiffusion coefficients were calculated from the amplitudes of sinusoidal distributions. The activation energy was determined to be 1.66 eV from the Arrhenius plot. The concentration-dependent interdiffusivity at 150°C was also estimated using Boltzmann-Matano method. The phase separation was observed in this material which has been known to be only homogenized. The annealing conditions turned out to be less than about 150 min at 180°C.

요 약 — 확산 현상은 박막성장 과정 및 박막의 기계, 전기, 자기적 성질 이해에 중요한 역할을 한다. 열처리에 의한 상호확산 때문에 생긴 Pd/Cu 다층박막의 조성변화를 AES depth-profiling 방법을 이용해서 조사하였다. 열처리된 시료에서의 각형의 초기 조성분포가 여러 온도에서의 열처리에 의해 정현파 모양의 조성분포로 변화되었다. 조성의존성을 고려하지 않은 상호확산 계수를 정현파 분포의 진폭으로부터 구하였으며, 1.66 eV의 값을 갖는 활성화에너지는 Arrhenius plot으로부터 산출하였다. 또한 Boltzmann-Matano 방법을 사용해서 150°C에서의 조성의존 상호확산 계수도 구하였다. 열처리에 의해 조성균일화가 되는 것으로만 알려졌던 본 물질계에서도 상분리가 생성됨을 관찰하였고, 그 열처리 조건은 180°C에서 150분 보다 짧아야함을 밝혔다.

1. Introduction

Multilayer (ML) thin films have been increasingly used in both basic researches and applications because of their specific physical properties that differ

from those of bulk materials and single-layer thin films [1, 2]. There are numerous and growing applications of ML thin films in communication, optoelectronics, hard and tribological coating, x-ray optical components [3], and high-density recording [4].

In many applications, one is often confronted with the undesirable effects arising from diffusion. Heat treatment or long-time use even at ambient condi-

*Present address: R & D Center, POSCON Corporation, P. O. Box 109, Pohang

**Author to whom all correspondences should be addressed

tions can lead to degradation of film structure. For example, in Mo/Si ML for x-ray mirror, increased broadening of the interfaces significantly reduces the reflectivity [5]. ML is known to have poor thermal stability in most cases.

Interdiffusion is one of generic topics in film science. Generally, thin films contain high-density low-temperature short circuits for diffusion, such as grain boundaries, dislocations and vacancies [6]. Diffusion coefficients in thin films are relatively high even at low temperatures. This means that, in thin film, the diffusion phenomenon is expected to present distinctive characteristics from bulk materials. Therefore, it is important to understand the diffusion behavior of thin film for both basic and applied aspects.

Diffusion stability is important especially for a ML film which is prepared to have abrupt interfaces. On annealing, the compositionally-modulated structure is changed to be either homogenized or phase-separated [6], and diffusion experiments are required to estimate complete homogenization time at a given temperature, or to estimate a device lifetime.

For the diffusion study of ML thin films, one requires techniques that can detect compositional variation in very short distance. Several techniques have been developed such as optical reflectivity, electrical resistivity [7], Rutherford backscattering [7], x-ray diffraction [8], Auger electron spectroscopy (AES), etc. Among those techniques, AES depth-profiling technique [9-11] has become one of the established methods.

2. Experiment

The Pd/Cu ML's were deposited onto Si wafers using an ultrahigh-vacuum physical vapor deposition system (Leybold L560UV). The deposition was achieved by alternating thermal evaporation of Pd (99.99%) and Cu (99.9%) at a base pressure of $2\sim 5 \times 10^{-7}$ torr. Alumina-overcoated tungsten boats were employed. The temperature was $30\sim 70^\circ\text{C}$ during the deposition. A single-crystal quartz sensor interfaced with XTC was installed to monitor the deposition rate and film thickness. Evaporation rate

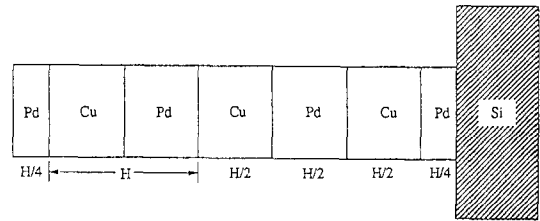


Fig. 1. Schematic structure of the prepared Pd/Cu ML thin film.

of Pd and Cu was $1.2 \text{ \AA}/\text{sec}$ and $1.3 \text{ \AA}/\text{sec}$, respectively.

The prepared ML films consist of three Cu layers and two Pd layers whose thickness is $H/2$ each, and of two boundary Pd layers of $H/4$, where H is the film periodicity of 1060 \AA . To preserve translational symmetry the thickness of the first and the last layer was made to be $H/4$ thick. A schematic structure of the prepared Pd/Cu ML is presented in Fig. 1. The total thickness of the ML was 3180 \AA , which was reconformed by an α -step (Tencor Instrument Model 200). The isothermal annealing at $150\sim 300^\circ\text{C}$ was performed in a vacuum furnace at a pressure of low 10^{-5} torr.

Composition depth profiles were acquired using a Perkin-Elmer (PHI) Auger system with 137 PC interface. The samples were etched with an inclined ($\sim 50^\circ$ from the surface normal) beam of 3- or 3.5-keV Ar ions, rastered over 3×3 or $4 \times 4 \text{ mm}^2$ on the surfaces. Most of the depth profiles were acquired in a continuous sputter mode. Sputtering rate was calibrated with Ta_2O_5 film of a known thickness, and the prepared Pd/Cu ML film whose total thickness was measured by α -step.

The Auger spectra for the elements to be monitored were registered as a function of the sputtering time by using a modified BLAES program. After a calibration of these data in terms of concentration and sputtered depth, respectively, composition depth profiles were obtained using Matlab program by Math Work.

3. Results and Discussion

3.1. Concentration-independent Interdiffusivity

The rectangular initial concentration profile of a

thin periodic ML film (ABABAB... structure) can be expressed as

$$c(x, 0) = \frac{1}{2} + \sum_{m=1}^{\infty} \frac{2}{\pi m} \sin\left(\frac{2\pi m x}{H}\right), \quad (1)$$

where x is the depth, and $m=1, 3, 5, \dots$.

After diffusion, it can be shown that the solution of Fick's second law in case of concentration-independent interdiffusivity (D) is another Fourier series, but with exponentially decreasing amplitudes

$$c(x, t) = \frac{1}{2} + \sum_{m=1}^{\infty} \frac{2}{\pi m} \exp\left[-\left(\frac{2\pi m}{H}\right)^2 Dt\right] \sin\left(\frac{2\pi m x}{H}\right). \quad (2)$$

For sufficiently long annealing times ($t \geq (0.3/D)(H/2\pi)^2$), the higher Fourier components decay very rapidly with time, and the amplitude of the sinusoidal distribution in Eq. (2) can be written as follows [6, 9-11];

$$\frac{1}{2} \frac{c_{\max} - c_{\min}}{c_{\max} + c_{\min}} = \frac{1}{2} (2c_{\max} - 1) \cong \frac{2}{\pi} \exp\left[-\left(\frac{2\pi}{H}\right)^2 Dt\right], \quad (3)$$

where c_{\max} is the maximum concentration of the element A inside layer A, and c_{\min} is the concentration of the element B at the same depth. $c_{\min} = 1 - c_{\max}$.

AES spectrum of an unannealed sample showed Pd peaks without any contamination by carbon and oxygen. On the other hand, we observed oxygen and carbon peaks on annealed samples, but these contaminants were able to be removed easily by sputtering of a few minutes.

AES depth profiling was carried out to obtain the concentration profiles along depth of Pd and Cu in both unannealed and annealed Pd/Cu ML thin films. The peak-to-peak heights in the first-derivative mode of the Pd MNN (302 eV), Cu LMM (916 eV) and O KLL (503 eV) transitions were successively measured in independent energy windows. Oxygen peak was monitored to check the impurity incorporation in the film. To convert the temporal variation of the measured Auger intensities to that of the composition we assumed that the relation

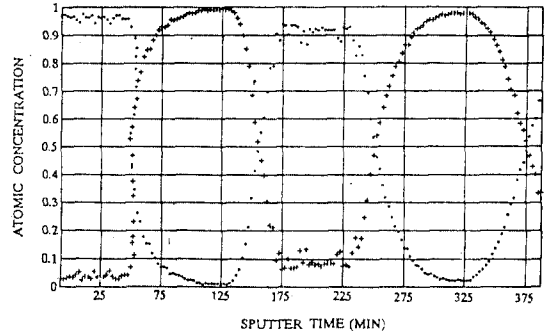


Fig. 2. Concentration profile of unannealed Pd/Cu ML. (*) denotes Pd and (+) Cu.

between Auger intensity and concentration was linear [14, 16].

Fig. 2 is the initial concentration profile, showing a rectangular concentration distribution. Once we have the sinusoidal concentration profiles for a thin ML film at an annealing temperature for various annealing times, we are able to estimate the interdiffusion coefficient at the temperature using Eq. (3). In Fig. 3 amplitude of the sinusoidal concentration distribution, $(2c_{\max} - 1)/2$, at various temperatures is plotted logarithmically against annealing time. The profiles are usually distorted by sputter-induced effects [14]. These undesirable effects give rise to degradation of depth resolution with increasing sputter depth and are most pronounced near the interface. On the other hand, the depth for c_{\max} is away from the interface. In addition, we made use of the value for c_{\max} in the top layer which was least distorted, therefore we could minimize the undesirable sputter-induced effects in determining the interdiffusion coefficient.

It should be noted that each data set in Fig. 3 follows a straight line, which verifies the exponential relation in Eq. (3). The absolute slope of the straight line increases with annealing temperature. This indicates a higher diffusivity at higher temperature. From the slopes of the straight lines the interdiffusion coefficients are calculated and listed in Table 1. At higher temperatures interdiffusion was so fast that the amplitude decreased to $c_{\max} \cong 0.5$ rapidly with annealing time, which means a completely homogenized concentration distribution. On the

Table 1. Interdiffusion coefficients of Pd/Cu ML

T(°C)	D(cm ² /sec)
165	1.2 × 10 ⁻¹⁷
180	5.8 × 10 ⁻¹⁷
195	1.5 × 10 ⁻¹⁶
210	8.2 × 10 ⁻¹⁶

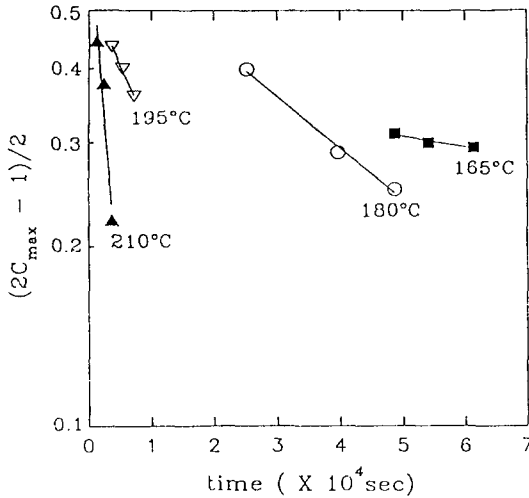


Fig. 3. Amplitude of the sinusoidal concentration distribution of Pd/Cu ML as a function of annealing time at various annealing temperatures.

contrary, at lower temperatures the concentration profile did not change significantly with annealing time.

The straight lines in Fig. 3 can be extrapolated approximately to the initial amplitude ($c_{max}=1$, i.e., $(2c_{max}-1)/2=0.5$) at $t=0$ except that at 165°C. This may be explained by that lattice diffusion was carried out at higher temperatures, while grain boundary diffusion was dominant at 165°C. We can classify the diffusion kinetics in a polycrystalline film into three cases (Fig. 4) [1, 2]. At low temperatures, virtually all of the diffusant is partitioned to grain boundaries (Fig. 4(a)). At elevated temperatures the extensive amount of lattice diffusion masks the penetration through grain boundaries (Fig. 4(c)). In between, the admixture of diffusion mechanisms results in an initial rapid penetration down the short-circuit network, which slows down as atoms leak into lattice (Fig. 4(b)). At 165°C in Fig. 3, a rapid

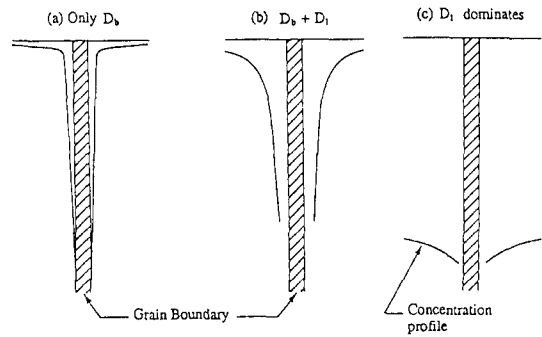


Fig. 4. Schematic penetration profiles of concentration according to the diffusion kinetics in a polycrystalline film: (a) grain boundary diffusion is dominant, (b) both grain boundary and lattice diffusion are comparable, and (c) lattice diffusion is dominant.

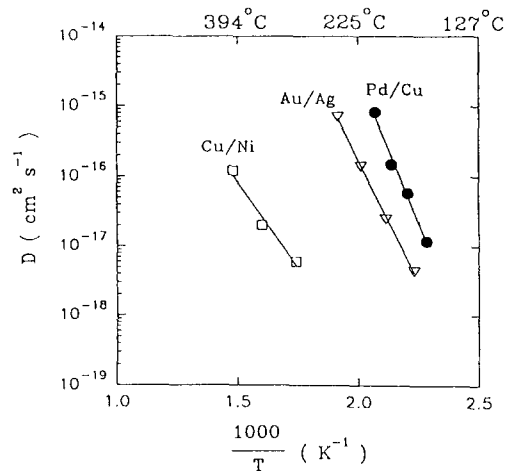


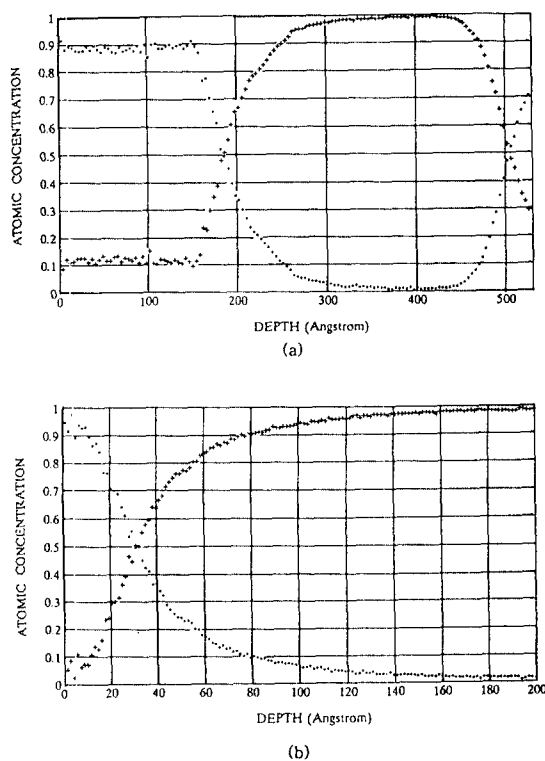
Fig. 5. Arrhenius plots of interdiffusion coefficients of various ML's.

diffusion proceeded probably through a higher density of grain boundaries in this sample at the beginning of annealing. At above 180°C, lattice diffusion controlled the diffusion rate, since the mean grain sizes are larger than about 50 nm [11].

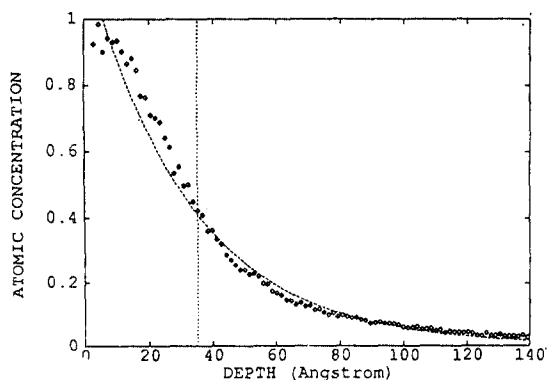
The interdiffusion coefficients obey the Arrhenius law. Figure 5 is Arrhenius plots of interdiffusion coefficients of Pd/Cu, Au/Ag [11] and Cu/Ni [9] ML. The data for Au/Ag and Cu/Ni ML from other works are included for comparison. The activation energy (E_a) for interdiffusion of Pd/Cu ML was determined to be 1.66 eV using the plot. D_0 (preexpo-

Table 2. Activation energies (in eV) of various ML's

	Pd/Cu	Au/Ag	Cu/Ni
Single-crystalline	2.12	1.95[16]	2.4[17]
	(coherent)[15]		
	2.88		
	(incoherent)[15]		
Polycrystalline	1.66	1.4[11]	1.1[9]
	(present case)		


Fig. 6. Concentration profile of Pd/Cu ML annealed at 150°C for (a) 120 min and (b) 300 min. (*) denotes Pd and (+) Cu.

nential constant) was 1.4×10^2 cm²/sec. Activation energies of various ML's are listed in Table 2 including that of the present polycrystalline Pd/Cu ML for comparison and summary. As can be seen in Table 2, the activation energies of polycrystalline films are smaller than those of the corresponding single-crystalline films. Very likely the reason is that it is due to the high density of defects existing in polycrystalline thin-film structures.


Fig. 7. Concentration profile of Pd down to a depth of 140 Å in Pd/Cu ML annealed at 150°C for 300 min, and fitted with an exponential function. (◇) denotes experimental data and dashed line fitting curve. Vertical line is called by Matano interface.

3.2. Concentration-dependent Interdiffusivity

When diffusion occurs in a large concentration gradient, the diffusivity should be considered as a function of concentration [2, 18]. In this case Fick's second law must be written in a general form as

$$\frac{\partial c}{\partial t} = \frac{\partial}{\partial x} \left(D \frac{\partial c}{\partial x} \right). \quad (4)$$

We can solve Eq. (4) to give

$$D(c') = - \frac{1}{2t} \left(\frac{dx}{dc} \right)_{c'} \int_0^{c'} x dc, \quad (5)$$

where x is the distance from the Matano interface and c' is an arbitrary concentration [2]. The Matano interface is defined as

$$\int_0^1 x dc = 0. \quad (6)$$

Eq. (5) indicates that measurement of c as a function of x gives D by the graphical method (Boltzmann-Matano method).

Fig. 6 shows concentration profiles of Pd/Cu ML annealed at 150°C. On annealing even for 300 min the profile was not changed into a sinusoidal but a nearly smooth spline form, which is satisfied with the condition of no interdiffusion extended to the top surface of the film. D can be calculated for a given concentration c' from Eq. (5) by fitting the

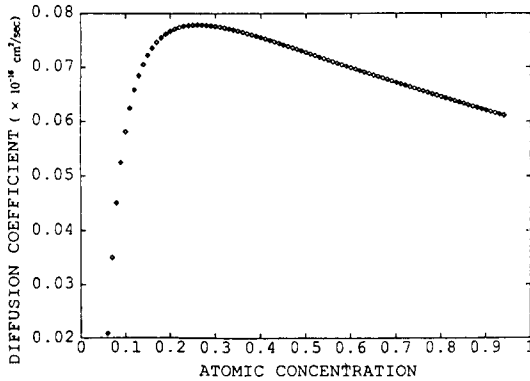


Fig. 8. Diffusion coefficient of Pd/Cu ML annealed at 150°C as a function of Pd concentration.

concentration profile of Pd in Fig. 6(b) with an exponential function (Fig. 7). $D(c')$ is computed reasonably in the range of $0.05 < c' < 0.95$, since the accuracy of the calculation falls off as c' becomes very close to either zero or unity [6]. The resultant diffusivity turned out to be strongly concentration-dependent as shown in Fig. 8. It is an averaged sum of the diffusivity of Pd and Cu. It is noted that the values of $D(c')$ are in the same order as that estimated independently of concentration (2.03×10^{-18} cm²/sec) even though the factors vary from 2 to 8 in case of concentration dependence considered.

3.3. Thermal Stability

When the artificial compositionally-modulated wavelength (CMWL) becomes extremely small, the gradient energy and strain effects must be considered. The modified diffusion equation is given by

$$\frac{\partial c}{\partial t} = D^{(1)} \frac{\partial^2 c}{\partial x^2} - D^{(2)} \frac{\partial^4 c}{\partial x^4}. \quad (7)$$

$$D^{(1)} = D \left(1 + 2\eta^2 \frac{Y}{f''} \right), \text{ where } \eta = \frac{\partial \ln a}{\partial c}.$$

$$D^{(2)} = D \left(\frac{2\kappa}{f''} \right), \text{ where } \kappa = N_v y d^2 \Delta V.$$

η is the change of the lattice parameter, a , with c , Y (modulus) a function of the elastic constants, f'' the second derivative of the free energy, and κ the gradient energy coefficient [19]. N_v is the number of atoms per unit volume, y bonds per atom, and d the distance between the planes. $\Delta V = V_{AB} -$

$(V_{AA} + V_{BB})/2$ where V_{AA} is the bond energy (a negative quantity) between two A atoms, V_{BB} that between two B atoms, and V_{AB} that between an A and a B atom. When κ (or ΔV) is negative, at all temperatures A - B bonds are preferred to A - A and B - B and the system has a tendency to order, i.e., to be homogenized. This also applies if κ (or ΔV) is positive when the temperature is high enough. At low temperature, however, the bond energy dominates, and it is favorable for the system to separate into two phases. In other words, the homogeneous system is unstable to arbitrarily small composition fluctuations; spinodal decomposition can occur. The spinodal decomposition is important because of its relation with the thermal stability of artificial modulated structures. In Eq. (7), $D^{(1)}$ contains the coherent strain contribution to the diffusivity, and $D^{(2)}$ contains the interfacial energy contribution to the driving force of diffusion.

The solution of Eq. (7) is similar to Eq. (2), replacing D of Eq.(2) by

$$D_\beta = D \left[1 + 2\eta^2 \frac{Y}{f''} + \frac{2\kappa}{f''} \beta^2 \right]. \quad (8)$$

It is apparent that the gradient energy contribution falls off rapidly with decreasing β ($=2\pi/H$) value and the contribution becomes negligibly small for long-wavelength concentration modulation.

On annealing ML thin films generally lower their free energy by reducing the high density of interfaces. Given sufficient atomic mobility, changes in the composition profile are expected to occur. There are steep concentration gradients at many interfaces in a ML thin film. If the ML is phase-separated, in other words, keeps a stationary-state concentration profile under practical annealing conditions, we can say that the ML is thermally stable. This kind of response is important especially for a ML whose prepared abrupt interfaces must be maintained even after a long-time thermal treatment such as thermomagnetic writing on a magneto-optical ML using a laser [1]. Au/Ni [6], Cu/Ni [6, 20], Fe/Cr [21] and Co/Cu [22] systems have been reported to show this phenomenon. This behavior was also observed in our Pd/Cu ML. Fig. 9 shows concentration profile of Pd/Cu ML annealed at 230°C for 90 min.

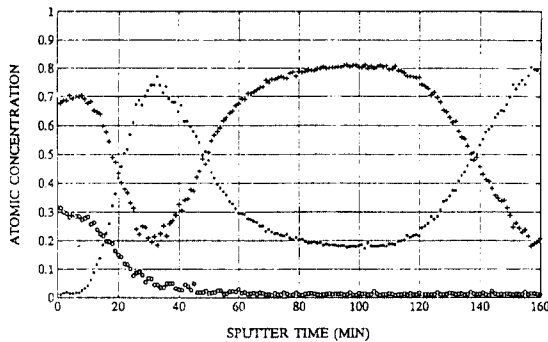


Fig. 9. Concentration profile of Pd/Cu ML annealed at 230°C for 90 min. (*) denotes Pd, (+) Cu, and (o) O.

The profile was not changed into a sinusoidal or homogenized distribution but still separated into two phases. The annealing condition which provides Pd/Cu system with this thermal stability at 180°C was investigated to be less than about 150 min. Phase-separating systems tend to lower their free energy further by coarsening[6]. The simplest continuous coarsening process is one in which there are thinning and thickening of alternate layers of a component, leading eventually to a doubling of the CMWL.

4. Conclusions

AES depth profiling was applied to study interdiffusion in polycrystalline Pd/Cu ML thin film at relatively low temperatures where the diffusion coefficients are small. It turned out that the method was very sensitive to measure those quantities.

At above 230°C diffusion was so fast that an almost homogeneous distribution was obtained. On the other hand, annealing experiments at 150, 165, 180, 195 and 210°C showed gradual sinusoidal changes in the concentration profiles according to the annealing time. The estimated concentration-independent diffusivity of the Pd/Cu ML allowed us to build up an Arrhenius plot and to extract the pre-exponential factor of 1.4×10^2 cm²/sec and the activation energy of 1.66 eV. This low activation energy indicates that the high density of defects such as dislocations, vacancies and grain boundaries, also

play important roles in my case as in other polycrystalline ML. On the contrary, this material system revealed larger activation energy than that of the polycrystalline Au/Ag and Cu/Ni ML. It may be ascribed to the observed phase separation.

The deterioration of the measured concentration profile due to the sputtering process was solved by taking the concentration amplitude at the top layer, but not the interfaces of the film in the determination of the concentration-independent diffusivities and the activation energy. However, the deteriorated profile was employed to obtain the concentration-dependent diffusivity using the Boltzmann-Matano method. Nevertheless, the values at 150°C are in the same order (10^{-18} cm²/sec) as that determined independently of concentration even though they are strongly dependent on concentration.

The layered structures disappear gradually or coarsen upon annealing. Coarsening (spinodal decomposition) system are more stable thermally than homogenizing systems. In all cases, a low interdiffusivity is desirable for the thermal stability. The phase separation was observed in the Pd/Cu ML which has been known to be only homogenized. The annealing conditions turned out to be less than about 150 min at 180°C.

The further investigation is required to understand the thermal stability and to analyze the coarsening quantitatively of Pd/Cu ML thin film in connection with phase separation. The microstructural measurement by, e.g., transmission electron microscope will be included in the investigation.

Acknowledgment

We would like to thank S. M. Chung and M. H. Kang for their many helpful discussions. This work was supported partially by the Korea Science and Engineering Foundation through the Advanced Materials Physics Research Center.

References

1. M. Ohring, *The Materials Science of Thin Films* (Academic Press, 1992).
2. K. N. Tu *et al.*, *Electronic Thin Film Science For*

- Electrical Engineers and Materials Scientists* (Macmillan Publishing Company, 1992).
3. D. G. Stearns *et al.*, *J. Vac. Sci. Technol.* **A9**, 2662 (1991).
 4. A. Fert *et al.*, *Magnetic Thin Films, Multilayers and Superlattice* (North-Holland, 1991).
 5. D. G. Stearns *et al.*, *J. Appl. Phys.* **67**, 2415 (1990).
 6. D. Gupta and P. S. Ho, *Diffusion Phenomena in Thin Films and Microelectronic Materials* (Noyes Publications, 1988).
 7. I. Suni *et al.*, *Thin Solid Films* **79**, 69 (1981).
 8. S. R. Teixeira *et al.*, *Appl. Phys.* **A48**, 481 (1989).
 9. K. Röhl and W. Reill, *Thin Solid Films* **89**, 221 (1982).
 10. W. Pamler, *Appl. Phys.* **A42**, 219 (1987).
 11. A. Bukaluk, *Appl. Surf. Sci.* **45**, 57 (1990).
 12. J. M. Walls, *Methods of Surface Analysis* (Cambridge, 1987).
 13. D. Briggs and M. P. Seah, *Practical Surface Analysis* (John Wiley & Sons, 1984).
 14. H. Oechsner, *Thin Film and Depth Profile Analysis* (Springer-Verlag, Berlin and Heidelberg, 1984).
 15. E. M. Philofsky and J. E. Hilliard, *J. Appl. Phys.* **40**, 2198 (1969).
 16. K. Meinel *et al.*, *Phys. Status Solidi* **A106**, 493 (1988).
 17. T. Van Dijk and E. J. Mittemeijer, *Thin Solid Films* **41**, 173 (1977).
 18. R. E. Reed-Hill, *Physical Metallurgy Principles* (Liton Educational Publishing, 1973), pp. 400-404.
 19. A. L. Greer and F. Spaepen, in *Synthetic Modulated Structures* (Academic Press, Inc., 1985), pp. 419-486.
 20. T. Tsakalakos, *Scripta Metall.* **15**, 255 (1981).
 21. H. Nakajima *et al.*, in *Proceedings of the 1st International Symposium on Metallic Multilayers* (Kyoto, Japan, March 1-5, 1993), p. 206.
 22. M. Doi and T. Miyazaki, in *Proceedings of the 1st International Symposium on Metallic Multilayers* (Kyoto, Japan, March 1-5, 1993), p. 195.